Archive of SID

Shahrood University of Technology
Iranian Society of Mining Engineering (IRSME)
Journal of Mining and Environment (JME)
journal homepage: www.jme.shahroodut.ac.ir
THOMSON REUTERS

Vol. 11, No. 1, 2020, 261-279.
DOI: 10.22044/jme.2020.9023.1789

Comparative and Competitive Study of LDH/Diatomite and Chitosan/Diatomite for Adsorptive Removal of Chloride Ion from Aqueous Solution

F. Sadough Abbasian[1], B. Rezai[2]*, A.R. Azadmehr[2], H. Hamidian-Shormasti[3]

1. Department of Mining Engineering ,Science And Research Branch,Islamic Azad University,Tehran,Iran
2. Department of Mining and Metallurgical Eng. Amirkabir University of Technology, Tehran, Iran
3. Department of Mining Engineering, Qaem Shahr Branch Islamic Azad University, Qaem Shahr, Iran

Received 13 October 2019; received in revised form 2 December 2019; accepted 7 January 2020

Keywords

Adsorption

Wastewater

Chloride

Anion exchange

Diatomite

Abstract

In this work, two clay-based composites are prepared for the adsorptive removal of the chloride ions from aqueous solutions. These composites are characterized through Fourier transform-infrared spectroscopy, scanning electron microscopy, X-ray fluorescence spectroscopy, and X-ray diffraction analysis. The effects of different parameters such as the contact time, amount of adsorbent, chloride concentration, temperature, and pH are studied by batch experiments. Also the isotherm, kinetic, and thermodynamic of the adsorptive removal of the chloride ions from these two composites are investigated. According to the results obtained, the adsorptive removal of chloride ions is initially rapid, and the equilibrium time is reached after 30 min. The optimal pH value is 7.0 for a better adsorption, and the maximum capacity can be achieved, which is 60.2 mg/g with 1000 mg/L of the initial chloride concentration. The Langmuir, Freundlich, Temkin, and Dubinin-Radushkevich adsorption models are applied to describe the equilibrium isotherms at different chloride concentrations. According to the equilibrium isotherms and the correlation coefficients (R2CDC: 0.9424, R2LDC: 0.996), the process can be described by the Langmuir model, and exhibits the highest removal rate of 97.24% (24.31 mg/g) with 250 mg/L of the initial chloride concentration. The pseudo-first-order and pseudo-second-order, intra-particle diffusion, and mass transfer kinetics models are used to identify the mechanism of the adsorptive removal of the chloride ions. The pseudo-second order model due the correlation coefficients (R2CDC: 0.9217-0.9852, R2LDC: 0.9227-0.9926) can be fitted to the kinetic calculations, and it is applicable for the adsorptive removal of chloride ions by the adsorbents. The thermodynamic calculations show that in a low chloride concentration, the sorption is spontaneous, associative, and endothermic; and in a high concentration, it is unspontaneous, dissociative, and endothermic. The calculated value of free energy (E) for adsorption onto the adsorbents suggests that the reaction rate controls the adsorptive removal of the chloride process rather than diffusion. It can be concluded that these two composites can be used as effective and applicable adsorbents for the adsorptive removal of chloride ions.

1. Introduction

In mining, water is used within a broad range of activities including mineral processing, dust suppression, slurry transport, and employee requirements. Over the last several decades, the industry has made much progress in developing close-circuit approaches that maximize water conservation. At the same time, the operations are often located in areas where there are not only significant competing municipal, agricultural, and industrial demands but also very different

Corresponding author: rezai@aut.ac.ir (B. Rezai).

www.SID.ir

Archive of SID

perspectives in the role of water culturally and spiritually. Recently, industrial wastewaters have been considered due to increment in the environmental impacts. Mining is one of the industries that produce wastewaters including ions such as chloride. Chloride ions increase the conductivity of water and the potential corrosivity [1–7]. Therefore, it is necessary to remove the undesirable pollution.

Several methods such as ion exchange, reverse osmosis, ultra-high lime with aluminum (UHLA) process, adsorption, Norcure, gas conditioning system, and electrochemical method are used for the removal of chloride ions [8]. As adsorption can be a simple, effective, and low- cost process, this makes it to become the most suitable process regarding pollution removal.

The low-cost process of water recovery is one of the most significant issues facing industry today. Therefore, natural materials can be a good choice as the potential adsorbents for chloride ion removal from aqueous solutions. Recently, different types of natural materials such as fique fibers [9], lime [10], and corn roots [11] have been studied for this purpose.

Also clay minerals have received much attention due to their abundance, availability, and low price. Various studies have been done using zeolite [12-14], bentonite [15-17], and kaolinite [18-20] as adsorbents. However, typically, natural clays have a low anion exchange capacity. Therefore, the adsorbent surface is usually modified in order to improve this feature.

Layered double hydroxide (LDH) as a class of synthetic anionic layered clays with a hydrotalcite-like structure containing positively charged metal hydroxide layers separated by anions and water molecules can be represented by the general formula of $[M^{+2}_{1-x}M^{+3}_{x}(OH)_2]^{x+}[A^{m-}_{x/m}]\cdot nH_2O$, where M^{+2} and M^{+3} are the divalent and trivalent cations, A^{m-} is the charge balancing interlayer anion, and x is the $M^{+3}/(M^{2+}+M^{3+})$ molar ratio (0.10 to 0.33) [21]. LDH is well-known as an excellent anion exchange material with broad applications but recently much more attention has been given to LDHs as an adsorbent [22-26]. Several studies have been done regarding anion adsorption using LDHs such as CaAl-LDH [27], MgFe-LDH [28], and ZnAl-LDH [29]. Therefore, using LDH in order to help a natural adsorbent and raise the adsorption capacity can be useful.

According to the chitosan special features as one of the most abundant natural polymers [30], there is a widespread use of chitosan as an adsorbent, especially in the removal of pollutants from wastewater [31-33].

Chitosan contains lots of —NH_2 and —OH groups in its molecule (Figure 1). It has a strong adsorption ability for many anions such as dyes (except for cationic dyes) due to its unique molecular structure [34]. However, normal chitosan has a small specific surface area, high cost, and low chemical stability, and would gel at a low pH value [35, 36], which limits its application in adsorption processes. Therefore, loading chitosan on another material can help to reduce the chitosan requirement and still keep the desired properties such as adsorption capacity.

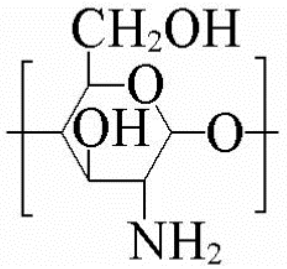

Figure 1. Structure of chitosan.

Diatomite is a lightweight sedimentary rock with a high porosity [37]. It is an inexpensive material, and can be found in many areas. Therefore, diatomite is an attractive immobilization material that may bring a new adsorbent with a high specific surface area and a strong adsorption ability for anions. Various studies have been carried out on the use of diatomite as an adsorbent for phosphate [38], fluoride [39], arsenic [40], and anionic dye [41, 42] removal from aqueous solutions.

The aim of this work was to prepare two clay-based composites by loading LDH and chitosan onto the raw diatomite (RD) via a co-precipitation method in order to improve the anion adsorption ability of diatomite. This is the first time that the adsorptive removal of chloride ions is evaluated by comparative and competitive studies with the two adsorbents LDH/diatomite clay (LDC) and Chitosan/Diatomite clay (CDC), which were specified by XRD, XRF, FT-IR, and SEM. The effects of different parameters such as the contact time, amount of adsorbent, chloride ion concentration, temperature, and pH were studied by batch experiments. Also the isotherm, kinetic, and thermodynamic of the adsorptive removal of chloride ions in LDC and CDC were investigated.

www.SID.ir

Archive of SID

2. Experimental

2.1. Materials

Mg $(NO_3)_2$-$6H_2O$, Al $(NO_3)_3$-$9H_2O$, acetic acid, and NaCl were supplied from Merck Company (Germany). All the water used was deionized. The chloride solution used was a synthetic wastewater prepared from anhydrous NaCl. Solution pH adjustment was carried out with 0.1 M NaOH and HNO_3, which were obtained from Merck Company (Frankfurt, Germany). Raw diatomite (RD) was obtained from the BDH chemical Ltd. company (England), and chitosan was obtained from Sigma–Aldrich Company (Germany).

Before use, all the adsorbents were milled, washed with distilled water, and oven-dried for 12 h at 80 °C. The dried adsorbents were stored in glass flasks.

Referring to the previous studies regarding the use of LDHs for chloride removal [4], Mg/Al LDH as the adsorbent with a significant adsorption capacity was selected and synthesized by applying a common co-precipitation method as follows: 0.15 mol Mg $(NO_3)_2 \cdot 6H_2O$ and 0.075 mol Al $(NO_3)_3 \cdot 9H_2O$ were dissolved in 150 mL of deionized water, thus forming a mixture solution. The solution was added dropwise into 50 mL of 2 M NaOH solution under vigorous stirring. The reaction mixture was heated at 60 °C for 3 h for aging. The precipitates obtained were centrifuged, washed with deionized water, and dried at 110 °C overnight.

2.2. Preparation of LDH/diatomite composite

MgAl-LDH was synthesized by the co-precipitation method at the constant pH of 11-12 and at a temperature of 80 °C [43]. A mixture of 1.50 mol/L Mg $(NO_3)_2$ and 0.75 mol/L Al $(NO_3)_3$ aqueous solution ($[M^{2+}]/[M^{3+}]$ = 2) was slowly introduced into a beaker containing 2 L distilled water and a clean RD. The water temperature was stably maintained at 80 °C with continuous heating and stirred for 4 h. During the addition, the pH of the solution was kept at 11∼12 using a 25% wt. NaOH solution. Then the slurry was aged at 80 °C for 12 h. The resulting precipitate was separated by centrifugation and washed for several times with deionized water to wash out all the dissolved salt. At last, the composites were dried in an oven at 100 °C for 16 h, giving the product MgAl-LDHs-RD.

2.3. Preparation of chitosan/diatomite composite

In this work, chitosan was used as the modification agent. In the primary experiment, the modified RD samples with different concentrations of chitosan (10, 30, 50 mg/g) were compared in order to find the most efficient and effective adsorbent. A higher concentration was not applied due to its too high stickiness during preparation. The results obtained showed that the modified RD with a higher chitosan concentration had a higher absorbance of chloride ions. Therefore, in this work, 50 mg/g was chosen as the modification concentration. The detailed preparation procedure is as follows: chitosan was dissolved in 5% (volume fraction) acetic acid solution at 50 g/L; 10 mL of this chitosan gel was added to 10 g of natural RD powder and mixed fast and sufficiently. This mixture was dried at 100 °C and ground into powder below 65 mesh for study. By this means, the modified RD powder studied in this work was obtained.

2.4. Physical measurements

The prepared adsorbents were specified by powder X-ray diffraction (Unisantis XMD 300, scan range 5°-70°), Fourier transform-infrared spectroscopy (NEXUS 870 FT-IR spectrometer range 500-4000 cm−1), scanning electron microscopy (Leo 440i SEM), and X-ray fluorescence spectrometers (Spectro Xepos). The solution pH adjustments were done by a pH-meter (827 pH lab, Metrhom, Swiss).

2.5. Batch adsorption experiments

Chloride solutions with different concentrations were prepared by diluting the stock solution with 10000 mg/L chloride concentration and used for the subsequent batch of adsorption experiments. In order to study the chloride removal process, 100 mL of chloride solution with concentrations ranged from 250 to 1000 mg/L was stirred at 500 rpm with each adsorbent (1 g) by changing the temperature from 25 °C to 70 °C. In order to specify the optimized contact time, the samples were collected at 5, 10, 15, 30, 45, 60, and 90 min. Also by adding HNO3 (0.1 mol/L) and NaOH (0.1 mol/L), the solution pH was adjusted. After equilibration, the remaining chloride ion content in the filtrate was measured by titrimetric analysis. Using the following equations, the ion removal percentage and uptake capacity could be calculated:

$$Removal\ \% = \frac{(C_0 - C_e)}{C_0} \times 100\% \quad (1)$$

$$q_e = \frac{(C_0 - C_e)V}{m} \quad (2)$$

www.SID.ir

Archive of SID

where C_0 (mg/L) and C_e (mg/L) are the initial and equilibrium chloride concentrations, respectively; q_e (mg/g) is the uptake capacity of chloride by adsorbent at equilibrium time; V (l) is the initial volume of solution; and m (g) is the mass of adsorbent.

In the isotherm experiments, 1 g of adsorbent was added to 100 mL chloride solutions with various initial concentrations ranging from 250 to 1000 mg/L. The mixtures were stirred for 30 min to reach equilibrium. The chloride concentrations of the supernatant solutions were determined. The chloride ion uptake by the adsorbent was calculated by the following equation:

$$q_t = \frac{(C_0 - C_t)V}{m} \quad (3)$$

where q_t (mg/g) is the uptake capacity of chloride by adsorbent at time t; V (l) is the volume of the solution; C_0 (mg/L) and C_t (mg/L) are the initial chloride concentration and chloride concentration at time t; and m (g) is the mass of adsorbent.

2.6. Equilibrium isotherms

The maximum adsorption capacity of chloride, surface properties of adsorbents, and mechanism of the adsorption process were characterized using the four different isotherm models Langmuir, Freundlich, Temkin, and Dubinin–Radushkevich (D–R); the related equations are shown in Table 1 [44-53].

Table 1. Equations of different isotherm models.

Model	Equation	Description	Ref.
Langmuir	$\frac{C_e}{q_e} = \frac{1}{Q_0 \times b} + \frac{C_e}{Q_0}$ $R_L = \frac{1}{1 + bC_e}$	q_e (mg/g): amount of adsorbed ion per unit weight of adsorbent C_e (mg/L): metal ion concentration in solution at equilibrium (after adsorption) b (L/mg): Langmuir isotherm constants Q_0: adsorption capacity, maximum in monolayer adsorption R_L: separation factor also called equilibrium parameter	[44-46]
Freundlich	$logq_e = logK_F + {}^{1}/_{n} logC_e$	K_F ($mg^{1-1/n}\ L^{1/n}\ g^{-1}$): Freundlich constants that display adsorption capacity of the adsorbent n (g/L): Freundlich constants that represent adsorption intensity (or surface heterogeneity) of the adsorbent	[47]
Temkin	$q_e = {}^{RT}/_{b} LnA + {}^{RT}/_{b} LnC_e$	b (J/mol): Temkin isotherm constants related to the heat of adsorption A: Temkin isotherm constant R: gas constant(8.314 J/mol K) T: absolute temperature	[50,51]
Dubinin-Radushkevich	$Lnq = Lnq_{max} - \beta R^2T^2Ln^2\left(1 + {}^{1}/_{C}\right)$ $E = {}^{1}/_{\sqrt{2\beta}}$	q_{max}(mg/g): capacity maximum of adsorption β(mol^2/KJ^2): a constant related to adsorption energy E: free energy per molecule of adsorbate (KJ) that represent: -If E < 8 kJ/mol: physical adsorption -If 8 < E< 16 kJ/mol: chemical absorption or ion exchange -For E > 16 kJ/mol : particle diffusion governs the reaction	[52,53]

By considering the shape of the isotherm, it can be predicted if the process is favorable or unfavorable. The R_L value can express the main features of the Langmuir isotherm, which can be calculated and interpreted as below [7, 54, 55]:

$$R_L = \frac{1}{1 + bC_0} \quad \begin{cases} RL > 1\text{: Unfavorable adsorption process} \\ R_L = 1\text{: Linear adsorption process} \\ 0 < RL < 1\text{: Favorable adsorption process} \\ R_L = 0\text{: Irreversible adsorption process} \end{cases} \quad (4)$$

www.SID.ir

Archive of SID

where C_0 (mg/L) and b (L/mg) are the initial chloride concentrations, respectively, and the Langmuir constant is related to the adsorption energy.

2.7. Kinetics studies

In the kinetic experiments, 100 mL of 1000 mg/L chloride solution with 1 g of adsorbent was stirred (500 rpm) for the selected times of 5 to 90 min, and then the adsorbent was filtered from the solution.

In order to identify the mechanism of the adsorptive removal of chloride, the kinetic results were applied to the reaction-based models, named pseudo-first-order and pseudo-second-order, and diffusion-based models, named intra-particle diffusion and mass transfer models. The theoretical aspects of the kinetic equations are shown in Table 2 [56, 57].

Table 2. Kinetic equations and parameters [56, 57].

Model	Linear equation	Equation	Parameters
Pseudo-first-order	$\ln(q_e - q_t) = lnq_e - K_1 t$	$\frac{d_{q_t}}{d_t} = K_1(q_e - q_t)$	q_t: amounts of ions adsorbed after t units of time q_e: amounts of ions adsorbed after time of reach to equilibrium (mg/g) K_1: pseudo-first order rate constant for the adsorption process (1/min)
Pseudo-second-order	$\frac{t}{q_t} = \frac{1}{K_2(q_e)^2} + \frac{1}{q_e}t$	$\frac{d_{q_t}}{d_t} = K_2(q_e - q_t)^2$	k_2: equilibrium rate constant of the pseudo-second-order equation (g/mg min).
Elovich	$q_t = \frac{1}{\beta}\ln(\alpha\beta) + \frac{1}{\beta}lnt$	$\frac{d_{q_t}}{d_t} = \alpha e^{-\beta q_t}$	α: initial adsorption rate (mmol/g min) β: related to the extent of surface coverage and the activation energy involved in chemisorption (g/mmol)
Intra-particle diffusion	$q_t = K_{pi}t^{1/2} + C_i$		K_{pi}: intra-particle diffusion rate constant of stage i (mg/g $min^{1/2}$) C_i: intercept of stage i
Mass transfer model	$q = B + \frac{1}{\beta}\ln(t)$ $B = \frac{\ln[k_{la}]_g - \ln\{ln\frac{C_0}{C_t}\}}{\beta}$ $[k_{la}]_f = [k_{la}]_g \times e^{-\beta lnq}$ $[k_{la}]_d = [k_{la}]_g - [k_{la}]_f$		B: potential mass transfer index β: (g min/mg) adsorbate–adsorbent affinity parameter $[k_{la}]_g$: global mass transfer factor $[k_{la}]_f$: film mass transfer factor $[k_{la}]_d$: internal diffusion factor

2.8. Thermodynamic studies

In the thermodynamic studies, 100 mL of chloride solution at various concentrations of 250, 600, and 1000 mg/L was stirred with 1 g adsorbent for 30 min at different temperatures (298, 323, 333, and 343 K).

The thermodynamic parameters can be calculated by the following equations:

$$\left.\begin{array}{l} q_e m = V(C_o - C_e) \\ K_d = {}^{q_e}/_{C_e} \end{array}\right\} \quad K_d = \frac{(C_0 - C_e)}{C_e} \times \frac{V}{m} \qquad (5)$$

where m and V are the amount of adsorbent (g) and the volume of solution (L), respectively. The Gibbs free energy of the process can be calculated as below:

$$\left.\begin{array}{l} \Delta G^0 = \Delta H^0 - T\Delta S^0 \\ \Delta G^0 = -RTlnK_d \end{array}\right\} \quad lnK_d = {}^{\Delta S^0}/_{R} - {}^{\Delta H^0}/_{RT} \qquad (6)$$

where ΔG^0 is the free energy of ion adsorption (kJ/mol), ΔH^0 is the heat of adsorption (kJ/mol), and ΔS^0 is the standard entropy change of adsorption (kJ/mol). According to the above equations, by having the adsorption distribution coefficient (K_d) values, ΔH^0 and ΔS^0 can be determined.

3. Results and discussion

3.1. Adsorbent characterization

The chemical composition of the samples is tabulated in Table 3. The most significant

www.SID.ir

Archive of SID

component of diatomite is SiO_2 (90.41 %). The high value of SiO_2 in the diatomite sample is consistent with the data obtained from the XRD analysis.

Table 3. Chemical composition of raw diatomite.

Oxide %	SiO_2	Al_2O_3	Fe_2O_3	CaO	MgO	K_2O	Na_2O	TiO_2	MnO	L.O.I
Diatomite	90.41	4.81	<0.1	<0.1	1.54	<0.1	1.13	<0.1	<0.1	2.11
CDC	49.25	3.24	<0.1	<0.1	1.15	<0.1	0.51	<0.1	<0.1	46.03
LDC	9.92	21.64	<0.1	<0.1	13.95	<0.1	12.56	<0.1	<0.1	41.93

The SEM microphotographs of the RD, CDC, and LDC samples are presented in Figure 2. It is clear that RD has a well-developed porous structure and looks like a circular sieve (Figures 2a and 2b). After loading with chitosan, the porous structure of the raw diatomite surface was still maintained, which provided a great possibility for chloride ions to be gathered and adsorbed (Figure 2c).

Figure 2d shows a well-prepared LDH with a typical plate-like structure. Also it could be recognized from Figure 2e that after making the composite, the diatomite surface was covered by LDH, and the porous structure of diatomite was not destroyed.

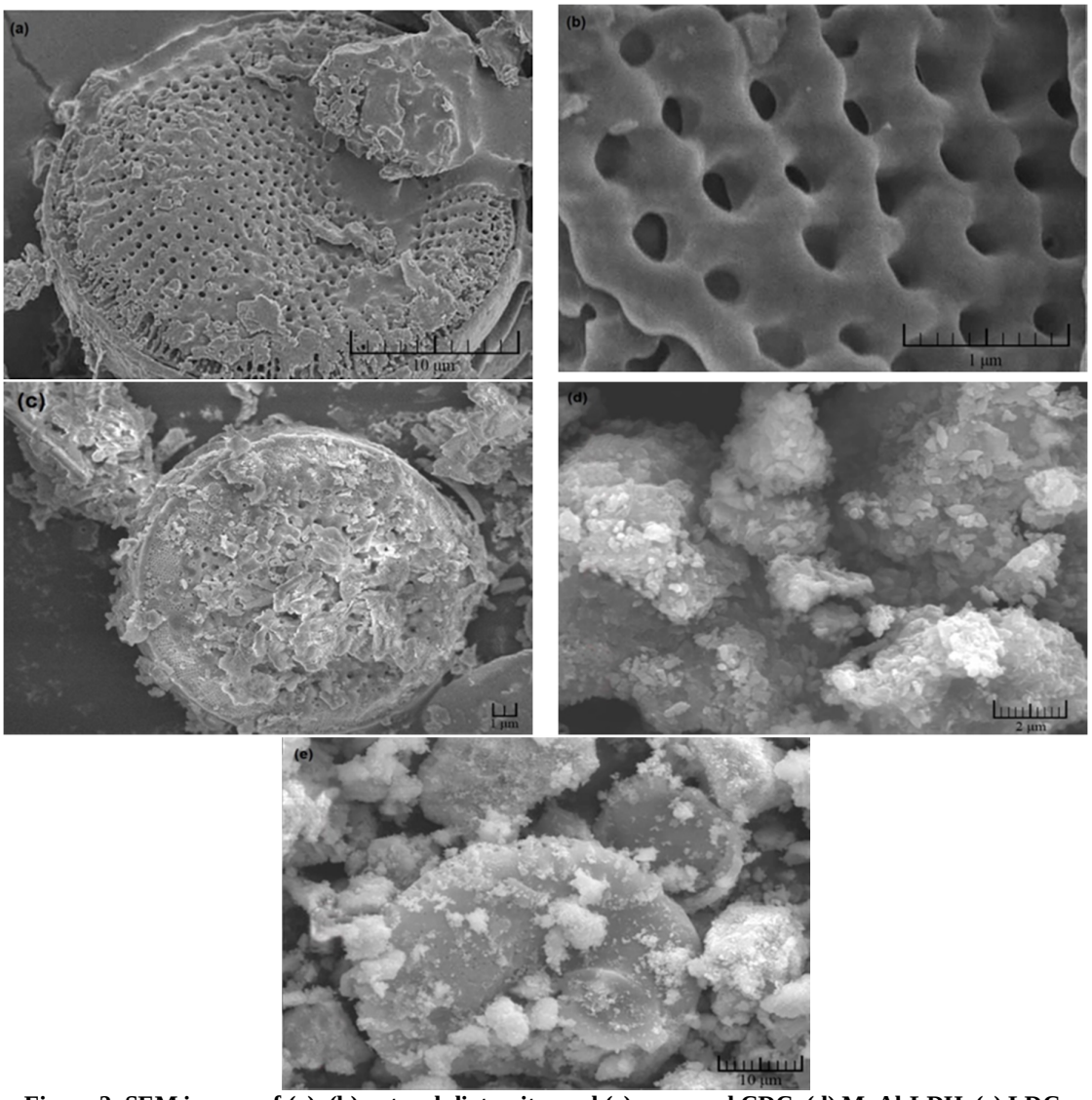

Figure 2. SEM images of (a), (b) natural diatomite, and (c) prepared CDC, (d) MgAl-LDH, (e) LDC.

www.SID.ir

Archive of SID

The FT-IR spectra for RD, CDC, and LDC are shown in Figure 3. The FT-IR spectrum for chitosan shows that the N—H and —OH stretching vibrations are overlapped around 3380 cm^{-1}. The C=O stretching vibration of the amide group and the bending vibration of the amine group can be indicated at 1655 cm^{-1} and 1595 cm^{-1} accordingly [58]. The characteristic glycoside absorption peak can be indicated at 1153 and 899 cm^{-1}. The band around 3380 cm^{-1} has been shifted to 3439 cm^{-1}, and the bands at 1595 cm^{-1} have been vanished, which indicate that the organic compounds containing nitrogen of chitosan are attached or adsorbed by diatomite [59]. According to Figure 3(c), the band at around 795 cm^{-1} corresponds to the free silanol group by diatomite. It can be confirmed by the results that chitosan is unified with diatomite [60-62].

According to Figure 3, the FT-IR spectra for LDC were compared with RC and LDH, which indicated the similarity of LDH and LDC. The stretching vibration of O-H can be indicated at 3439 cm^{-1}, which is related to hydroxyl groups and water molecules. The peak at 1650 cm^{-1} is related to the H_2O bending vibration [63]. The peak at 1390 cm^{-1} is related to NO_3^- in the inter-layer. The band around 1091 cm^{-1} confirms the existence of the Si-O stretching [64]. The bands observed between 500-800 cm^{-1} can be assigned to the lattice vibration models of M—OH and M—O.

Figure 4 shows the XRD patterns of the samples. According to Figure 4(a), the main peaks of diatomite are observed at 21.8°, 28.2°, 31.3°, and 36.0° (2θ); the peak at 21.8° reflects SiO_2 [65].

According to Figure 4(b), the observed peaks at 10.6° and 20.4° are related to chitosan [66]. Although no shifts could be observed, the peaks were weakened. This is probably due to the easy dispersing of diatomite in the chitosan solution in order to form a desirable inter-play with chitosan.

The XRD patterns for LDH and LDC are shown in Figures 4c and 4d. Typically, LDH shows the reflection peaks around 9°, 32°, 34°, 37°, 47°, 56°, and 62°, corresponding to the planes (003), (101), (009), (015), (012), (110), and (113), respectively, which are typically related to hydrotalcite [65-68]. It is obtained from the figure that the peak around 9° starts to appear on the LDC sample, which indicates that LDH is well-formed. It can be specified from the results that during the loading process, nothing changed in the LDH structure.

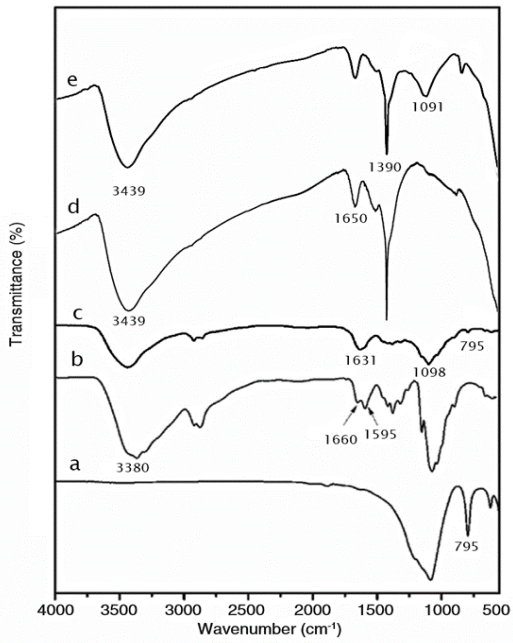

Figure 3. FT-IR spectra for (a) diatomite, (b) chitosan, (c) CDC, (d) MgAl-LDH, and (e) LDC.

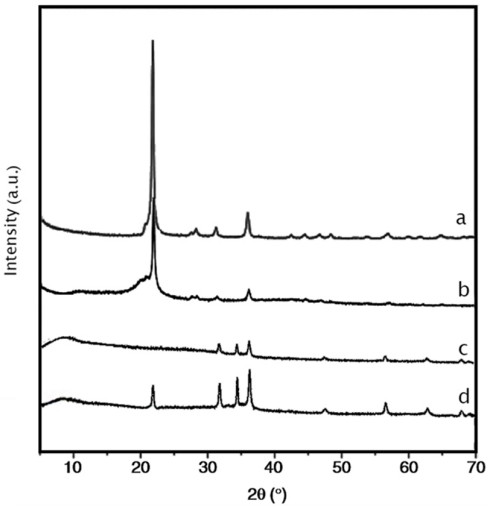

Figure 4. XRD patterns for (a) diatomite, (b) CDC, (c) MgAl-LDH, and (d) LDC.

3.2. Effect of contact time

The adsorptive removal of chloride ions was studied with the contact time ranged from 5 to 90 min. The experiments were done using 1 g of adsorbents mixed in 100 mL of chloride solutions (1000 mg/L). It can be seen in Figure 5 that by increasing the time from 5 to 30 min, the chloride removal increases, and thereafter, will not change significantly. The maximum adsorptive removal of chloride ions by LDC and CDC is 52% and 59.5% in 90 min with a 1000 mg/L chloride ion concentration and 1 g adsorbent.

www.SID.ir

Archive of SID

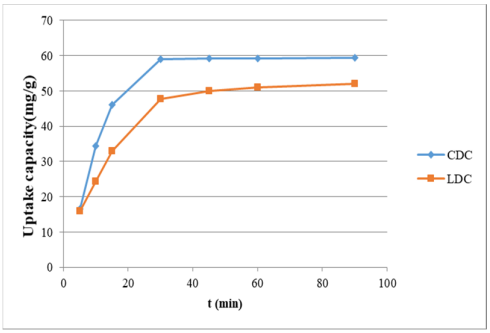

Figure 5. Relationship between the chloride uptake capacity by CDC and LDC and the time (C_0 = 1000 mg/L, T = 25 °C, adsorbent amount = 1 g).

3.3. Effect of amount of adsorbents

Figure 6 shows the effect of the amount of adsorbent on the adsorptive removal of chloride ions. It shows that by increasing the amount of adsorbent, the percentage of chloride removal increases, which can demonstrate that more sections are susceptible to absorption. It can be seen in the figure that by increasing the amount of adsorbent to more than 1 g, the removal percentage does not significantly change. However, it can be seen in Fig. 6 that by increasing the amount of adsorbent, the adsorption efficiency increases but the amount adsorbed per unit mass decreases. It can be understood that the number of available adsorption sites increases by increasing the amount of adsorbent but the drop in the adsorption capacity is basically due to the sites remaining unsaturated during the adsorption process. In other words, the decrease in the adsorption capacity is basically due to masking of the adsorption sites, i.e. the available surface area for chloride adsorption decreases due to aggregation of the active sites for adsorption.

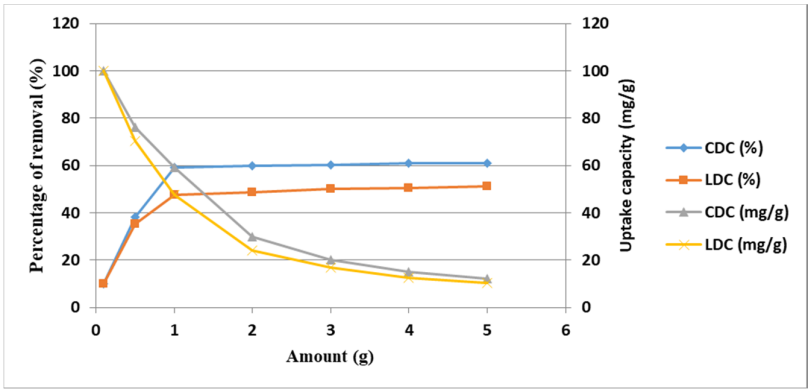

Figure 6. Relation between percentage of removal and different amounts of adsorbent.

3.4. Effect of solution pH

In order to investigate the effect of pH on the adsorptive removal of chloride by LDC and CDC, the batch experiments were done with different pH values (2.0-12.0). Figure 7 shows that by adjusting the pH value to 7.0, the maximum capacity can be achieved, which is 60.2 mg/g for CDC and 47.7 mg/g for LDC.

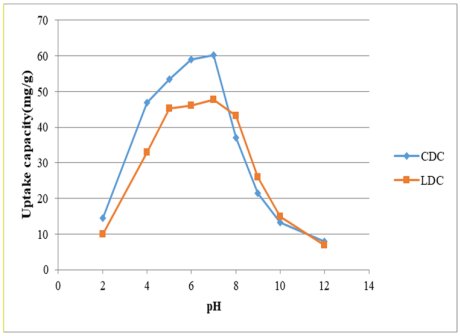

Figure 7. Relation between adsorption capacity and different pH values.

As a result, in the range of 5.0-8.0 for the LDC adsorbent, the pH impact was not insignificant. However, for all values outside this range, the uptake capacity of chloride ions was decreased. This can be related to OH^- increase when pH value is higher than 8.0. By reducing the pH value to lower than 5.0, dissolving the metal cations of LDHs will start, which reduces the uptake capacity. Also by decreasing the pH value of the solution, there are more nitrate ions in the solution, which prevent the chloride ion exchange. For CDC, the pH of the solution has a significant impact on the process. It was found that by adjusting the pH value of the solution at 7.0, the highest adsorption capacity of chloride could be achieved. As shown in Figure 7, the optimum pH was frequently reported around pH 4–7. At a lower pH, chitosan is soluble in water, which causes decreasing the activated sites on the surface.

www.SID.ir

Archive of SID

Also at low pH values, H^+ increases on the CDC surface, which causes an electromagnetic force formation between the chloride ions and the adsorbent surface [69]. By increasing the pH value of the solution, OH^- increases, which competes with chloride ions for adsorption.

3.5. Effect of chloride ion concentration

In order to show the effect of the initial solution concentration on the adsorptive removal of chloride ions, the batch experiments were studied with different concentrations (250, 400, 500, 600, 750, and 1000 mg/L). Figure 8 shows that the adsorption loading increased from 5 to 30 min, and thereafter, it remained almost constant. Chloride ions were almost totally adsorbed at 250 mg/L. By increasing the initial solution concentration, the uptake capacity increased. This increase is attributed to the fact that as the concentration increases, the number of collisions between the chloride ions and the adsorbents increases due to the increase in the mobility of the ions because of high collisions between the ions themselves. The initial chloride concentration creates an important driving gradient force to overcome the mass transfer resistance to anions between the solid and aqueous phases. The data showed that the chloride adsorption capacity of CDC and LDC increased from 24 to 59.5 mg/g and from 24 to 52 mg/g with chloride concentration increasing from 250 to 1000 mg/L (Figure 8). This could be due to a high mass transfer force. However, the chloride percent removal decreased from 96% to 59.5% and from 90.8% to 52% for CDC and LDC, respectively, due to the saturation of the binding sites on the adsorbents.

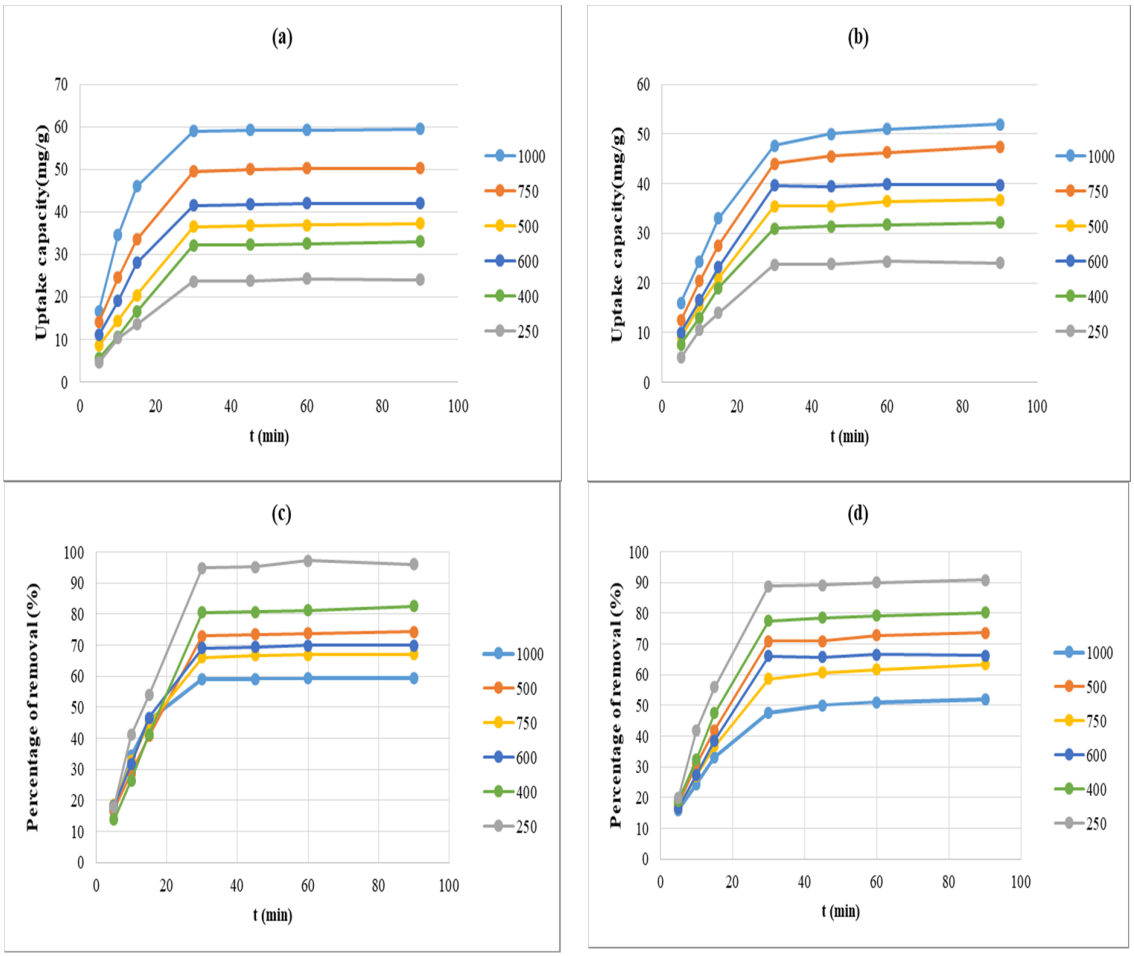

Figure 8. (a). Relation between adsorption capacity and different initial chloride concentration for CDC. (b). Relation between adsorption capacity and different initial chloride concentration for LDC. (c). Relation between percentage of removal and different initial chloride concentration for CDC. (d). Relation between percentage of removal and different initial chloride concentration for LDC.

www.SID.ir

Archive of SID

3.6. Adsorption equilibrium studies

In order to determine the optimum conditions for the adsorptive removal of chloride ions, the equilibrium studies for the Langmuir, Freundlich, Temkin, Dubinin– Radushkevich (D–R) models were carried out.

The homogeneous mono-layer adsorption of the ions onto the surface with a limited number of adsorption sites is defined by the Langmuir model [44-46].

It can be seen in Table 4 that the results obtained can be applied to the Langmuir model, showing a better fit than the others for both CDC and LDC according to the correlation coefficients (R^2_{CDC}: 0.9424, R^2_{LDC}: 0.996). The R_L values for the initial concentrations of chloride ions between 250 and 1000 mg/L were calculated for both CDC and LDC as 0.0657-0.2196 and 0.0538-0.1855, respectively. Therefore, as the R_L value is between 0 and 1, the adsorptive removal of chloride ions is favorable and reversible.

The heterogeneous faces can be explained using the Freundlich model, which indicate a favorable adsorption by obtaining n as the Freundlich constant between 1 and 10 [47].

Table 4 shows that n for CDC and LDC is 4.29 and 2.063, and according to the correlation coefficient (R^2) values 0.9349 and 0.9954, the process can also be described well by the Freundlich model.

The revised form of the Langmuir model by adding the temperature impact on the process called the Temkin model was studied [50, 51].

According to Table 4 and due to the correlation coefficient (R^2) values, temperature does not have a positive effect on the chloride homogeneous adsorption onto CDC.

Using the Dubinin–Radushkevich model, the physical or chemical nature of the adsorption process can be specified [52, 53].

The E value is used to ascertain the type of adsorption process under consideration. If the adsorption energy is E < 8 kJ/mol, the adsorption would be done physically. For chemical absorption or ion exchange, the adsorption energy would be 8 < E < 16 kJ/mol, while for the values of E > 16 kJ/mol, the particle diffusion controls the process [52]. Thus as the adsorption free energies (E) for CDC and LDC are 13.168 KJ and 10.234 KJ, respectively (Table 4), the process is controlled by chemical absorption or ion exchange.

The correlation coefficient value (0. 9794) for the adsorption of chloride ions onto LDC shows a good fit, while the value of correlation coefficient for CDC (0.8935) reduces validity, which has been mentioned above.

Table 4. Langmuir, Freundlich, Temkin, and Dubinin–Radushkevich isotherm constants for chloride adsorption.

Model	Parameter	CDC	LDC
Langmuir	R^2	0.9424	0.996
	q_m (mg/g)	63.291	52.356
	b	0.0142	0.0176
	R_L	0.0657-0.2196	0.0538-0.1855
Freundlich	R^2	0.9349	0.9954
	n (g/L)	4.0290	2.7203
	K_F ($mg^{1-1/n}$ $L^{1/n}$ g^{-1})	11.7138	4.2855
Temkin	R^2	0.8416	0.9441
	b (J/mol)	270.8469	255.7494
	A (L/mg)	0.6623	0.1279
Dubinin–Radushkevich	R^2	0.8935	0.9794
	β (mol^2/KJ^2)	2.88×10^{-9}	4.77×10^{-9}
	E (KJ)	13.1681	10.2348
	q_m (mg/g)	0.0012	0.0013

3.7. Adsorption kinetics studies

As mentioned in Section 3.2, Figure 5 shows that the chloride ion removal increases by increasing time and reaches the optimum time at 30 min, and thereafter, remains almost constant.

The kinetic models such as pseudo-first-order, pseudo-second-order, intra-particle diffusion, Elovich, and mass transfer were examined in order to determine the effective processes

www.SID.ir

Archive of SID

regarding the adsorptive removal of chloride ions on CDC and LDC.

The rate constant of the adsorption process can be calculated from the plot of $\ln(q_e-q_t)$ vs. t (Tables 5 and 6). The results obtained show that due to the low R^2 values, the pseudo-first-order model is not suitable for describing the experimental data.

The experimental data was assessed for the pseudo-second-order model. Tables 5 and 6 show the related values of k_2 and q_e, which are obtained from the t/q_t vs. t plots. The linear plots are shown in Figure 9 at different initial chloride ion concentrations, which indicate that this model is applicable for the adsorptive removal of chloride ions by CDC and LDC. Tables 5 and 6 show that by using this model, the calculated q_e values are close to the experimental data, and the high R^2 values indicate that the adsorptive removal of chloride follows a second-order. Describing the chloride ion adsorption mechanism by this model corroborates chemisorption and ion exchange.

The intra-particle diffusion and mass transfer models were investigated and the results obtained were tabulated in Table 7. Generally, external diffusion and internal diffusion or a combination of them can control the adsorption process

According to Table 2 and considering the related equation of the intra-particle model, q_t vs. $t^{1/2}$ was plotted. The intra-particle can be considered as the only controlling step of the process if the drawing linearly passes through the origin; otherwise, the presence of other mechanisms is also confirmed [70].

Figure 10 shows two different linear parts for both CDC and LDC, which indicate different rates of mass transfer in the macro-pore (stage 1) and micro-pore (stage 2) diffusions. It can be seen in Table 7 that the adsorptive removal of chloride ions onto CDC has the highest k_{p1} value, while in the second stage of the process, the highest value of k_{p2} is related to LDC, which indicates that the adsorptive removal of chloride ions onto CDC is mostly controlled by film diffusion, while for LDC, the intra-particle diffusion is dominated.

According to the stages 1 and 2 of the process, the change in the intra-particle diffusion rate from fast to slow can be explained by the limited desirable surface and lower chloride content in the second stage.

The origin is not cut-off by the plot, as it can be seen in Table 7, and the presence of other mechanisms is confirmed accordingly.

According to Table 7, an idea can be obtained about the boundary layer thickness by having the intercept values [71]. The results for both stages show that the adsorptive removal of chloride ions by CDC has the highest C_i value, which confirms the greater effect of the boundary layer.

The mass transfer resistance investigation can help to specify the adsorption mechanisms more accurately. Using the mass transfer model, the extent of the porosity and the adsorbent bed thickness that affect the adsorption capacity can be determined.

Based on the mass transfer equations in Table 2, the internal diffusion $[k_{la}]_d$, film mass transfer $[k_{la}]_f$, and global mass transfer $[k_{la}]_g$ factors as the mass transfer parameters were determined. It can be calculated from the plot of mass transfer factors vs. C_e/C_0% (Figure 11) that the rate of factors decrease by increasing the C_e/C_0 value. This indicates the surface impregnation of CDC and LDC with chloride ions during the process.

It can be concluded that the rate of chloride mass transfer to CDC is faster than LDC due to the greater variation in the mass transfer factors for CDC. Also $[k_{la}]_f > [k_{la}]_d$, which shows a greater effect of the rate of film diffusion on the adsorptive removal of chloride ions.

As it can be seen in Tables 5 and 6, the Elovich equations did not fit well to the experimental data. Therefore, this model is not applicable for describing the experimental data.

Table 5. Kinetic parameters for the adsorption of chloride ions onto CDC.

C_0 (mg/L)	q(exp) (mg/g)	First-order kinetic eq		Second-order kinetic eq			Elovich eq.		
		K_1(1/min)	R^2	q_2(mg/g)	K_2 (g/mg min)	R^2	α (mmol/g min)	β (g/mmol)	R^2
0.9088	0.9055	0.9059	0.9011	0.9058	0.8675	0.9088	0.9055	0.9059	0.9011
0.1329	0.091	0.0876	0.0844	0.0728	0.0666	0.1329	0.091	0.0876	0.0844
3.2273	3.6977	5.0411	11.8574	9.4402	14.6232	3.2273	3.6977	5.0411	11.8574
0.9506	0.9217	0.9663	09797	0.9845	0.9852	0.9506	0.9217	0.9663	09797
0.0027	0.0015	0.0018	0.0022	0.0019	0.0019	0.0027	0.0015	0.0018	0.0022
25.6155	35.4526	39.2277	43.9282	52.3499	61.3413	25.6155	35.4526	39.2277	43.9282

www.SID.ir

Archive of SID

Table 6. Kinetic parameters for the adsorption of chloride ions onto LDC.

C_0 (mg/L)	q(exp) (mg/g)	First-order kinetic eq		Second-order kinetic eq			Elovich eq.		
		K_1(1/min)	R^2	q_2(mg/g)	K_2 (g/mg min)	R^2	α (mmol/g min)	β (g/mmol)	R^2
0.1506	0.1049	0.0926	0.0848	0.0743	0.0729	0.1506	0.1049	0.0926	0.9113
3.5074	4.645	5.3981	5.9738	7.2695	9.6794	3.5074	4.645	5.3981	0.9113
0.9724	0.9744	0.9782	0.9227	0.9862	0.9926	0.9724	0.9744	0.9782	0.9113
0.003	0.0023	0.002	0.002	0.0016	0.0018	0.003	0.0023	0.002	0.9113
23.7932	33.6612	38.3763	41.8254	49.1347	53.3523	23.7932	33.6612	38.3763	0.9113
0.8101	0.8533	0.8169	0.6901	0.9463	0.9252	0.8101	0.8533	0.8169	0.9113

Table 7. Intra-particle diffusion model parameters for the adsorption of chloride by 1 g of adsorbent; conditions: initial chloride concentration: 1000 mg/L, speed stirrer: 500 rpm, temperature: 298 K.

Adsorbent	Intra-particle diffusion					
	K_{p1} (mg/g $min^{1/2}$)	C_1	R_1^2	K_{p2} (mg/g $min^{1/2}$)	C_2	R_2^2
CDC	12.8320	-8.3116	0.9486	0.1220	58.3530	0.9894
LDC	9.8841	-6.1939	0.9973	1.0384	42.5380	0.9165

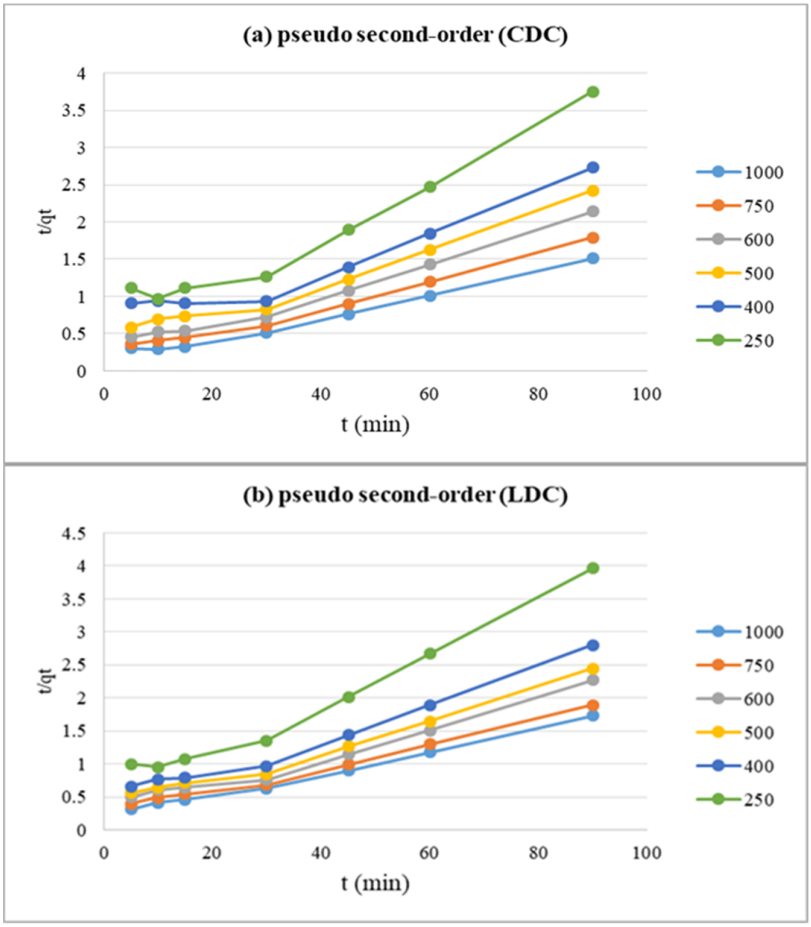

Figure 9. Pseudo-second-order rate expression for the adsorption of chloride by 1 g of (a) CDC and (b) LDC at various initial concentrations; conditions: speed stirrer: 500 rpm, temperature: 298 K.

www.SID.ir

Archive of SID

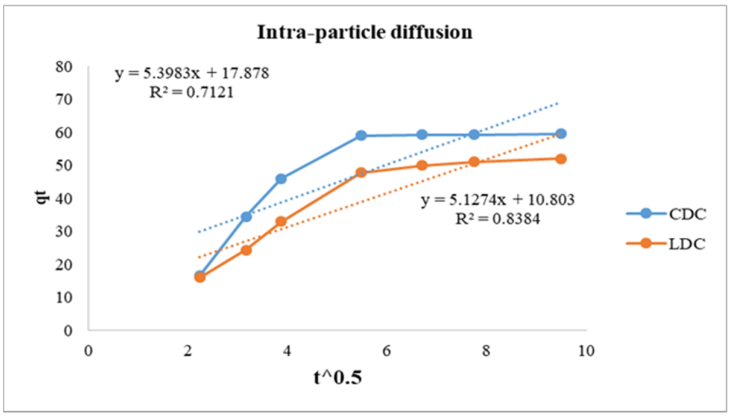

Figure 10. Intra-particle diffusion model for the adsorption of chloride by 1 g of (a) CDC and (b) LDC; conditions: initial chloride concentration: 100z0 mg/L, speed stirrer: 500 rpm, temperature: 298 K.

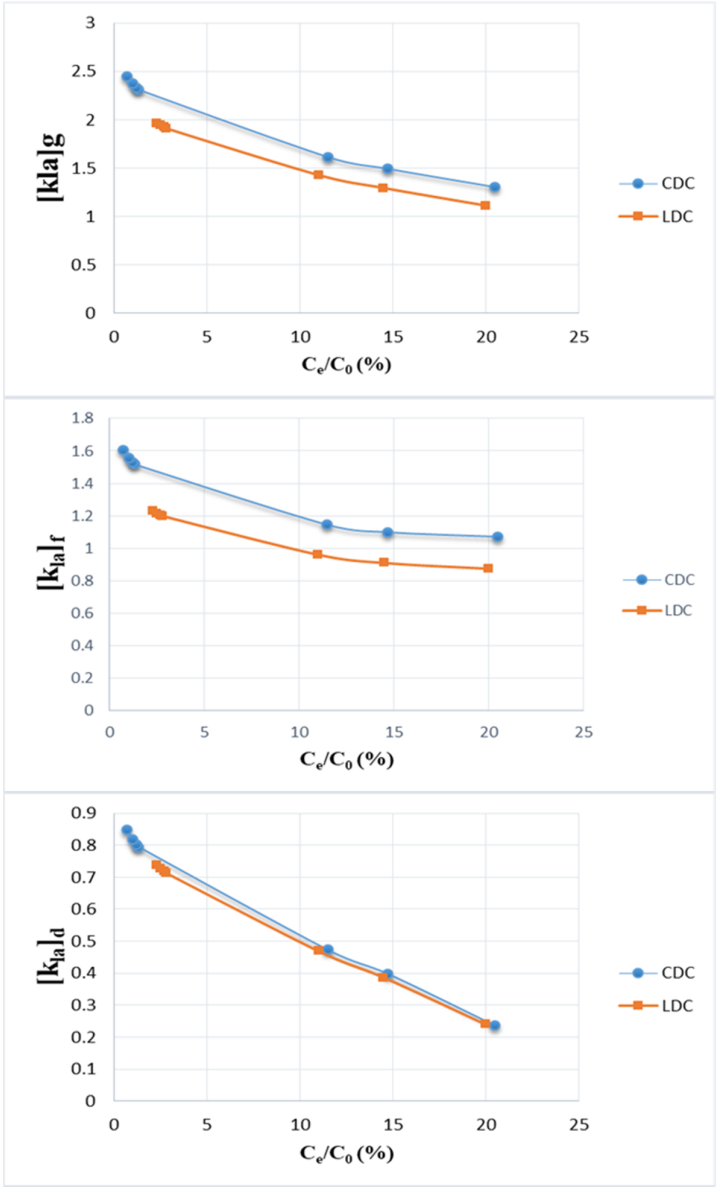

Figure 11. Variation in mass transfer factors: (a) $[k_{la}]_g$, (b) $[k_{la}]_f$, (c) $[k_{la}]_d$ for chloride ion adsorption onto CDC and LDC (C_0 = 250 mg/L, T = 25 °C, amount of adsorbent = 1 g).

www.SID.ir

Archive of SID

3.8. Adsorption thermodynamic studies

In order to determine the thermodynamic parameters, as it is shown in Figure 12, ΔH° and ΔS° can be calculated by plotting $\ln K_d$ vs. 1/T. Tables 8 and 9 demonstrate the thermodynamic parameters for chloride ion adsorption.

Table 8. Thermodynamic parameters for the adsorption of chloride ions onto CDC.

Adsorbent	C_0 (mg/L)	ΔH^0 (KJ/mol)	ΔS^0 (KJ/mol)	ΔG^0 (KJ/mol)			
				298 K	323 K	333 K	343 K
CDC	250	1.9405	0.0115	-1.4878	-1.7923	-1.8959	-2.0031
	600	9.0814	0.0166	3.7031	3.9081	3.4790	3.3052
	1000	4.3843	-0.0016	4.8031	5.0385	4.8657	4.8634

Table 9. Thermodynamic parameters for the adsorption of chloride ions onto LDC.

Adsorbent	C_0 (mg/L)	ΔH^0 (KJ/mol)	ΔS^0 (KJ/mol)	ΔG^0 (KJ/mol)			
				298 K	323 K	333 K	343 K
LDC	250	11.0352	0.0215	4.5626	4.2924	3.8752	3.5528
	600	3.3598	-0.0158	8.0489	8.5427	8.6370	8.7397
	1000	2.1671	-0.0261	9.9204	10.6666	10.8639	11.0761

For chloride ion adsorption onto CDC at a low concentration (250 mg/L), the spontaneous adsorption process can be explained by negative ΔG° values. According to the results shown in Table 8, by increasing the temperature from 298 K to 343 K, the ΔG° values also increase, which means that the adsorptive removal of chloride ions can spontaneously increase. The positive values of ΔG° at high concentrations (600, 1000 mg/L) show that although the process is feasible, it is not spontaneous. By increasing the temperature from 323 K to 343 K, ΔG° decrease, which shows that at higher temperatures the process becomes more favorable [7].

The positive ΔH° values confirm that the adsorptive removal of chloride ions is an endothermic process and the adsorption of chloride ions on to CDC can be increased by increasing the temperature.

The positive ΔS° changes at lower chloride concentrations (250 and 600 mg/L) show that an associative process occurs in the chloride adsorption. The negative ΔS° value at a high concentration (1000 mg/L) reflects that no significant diffusion of ions occurs.

According to Table 9, for chloride ion adsorption onto LDC, the positive ΔG° values show that although the process is feasible, it is not spontaneous. By increasing the temperature at a low concentration (250 mg/L), ΔG° decreases, which shows that at higher temperatures, the process becomes more favorable. According to the results obtained for high concentrations, by increasing the temperature, the ΔG° values increase, which indicate that the adsorptive removal of chloride ions is an unspontaneous process. Unspontaneous reactions can occur but require an external energy source. Hence, in this work, as the solution is stirred using a magnetic stirrer at 500 rpm, it helps to overcome the difficulty of the process. Thus as the process is kinetically controlled, adsorption can occur at ordinary temperatures, even though it is thermodynamically unstable. Therefore, it seems that the lower amount of chloride ions adsorbed on the LDC is due to this reason.

The positive ΔH° values confirm that the adsorptive removal of chloride ions is an endothermic process and the adsorption of chloride ions onto LDC can be increased by increasing the temperature.

The ΔS° value at a low chloride concentration (250 mg/L) that is positive shows that an associative process occurs in chloride adsorption by LDC. This also indicates that during the process, LDC is affined to chloride ions and structural changes occur [7]. The negative changes of ΔS° value at high concentrations (650 and 1000 mg/L) reflect that no significant diffusion of ions occurs.

www.SID.ir

Archive of SID

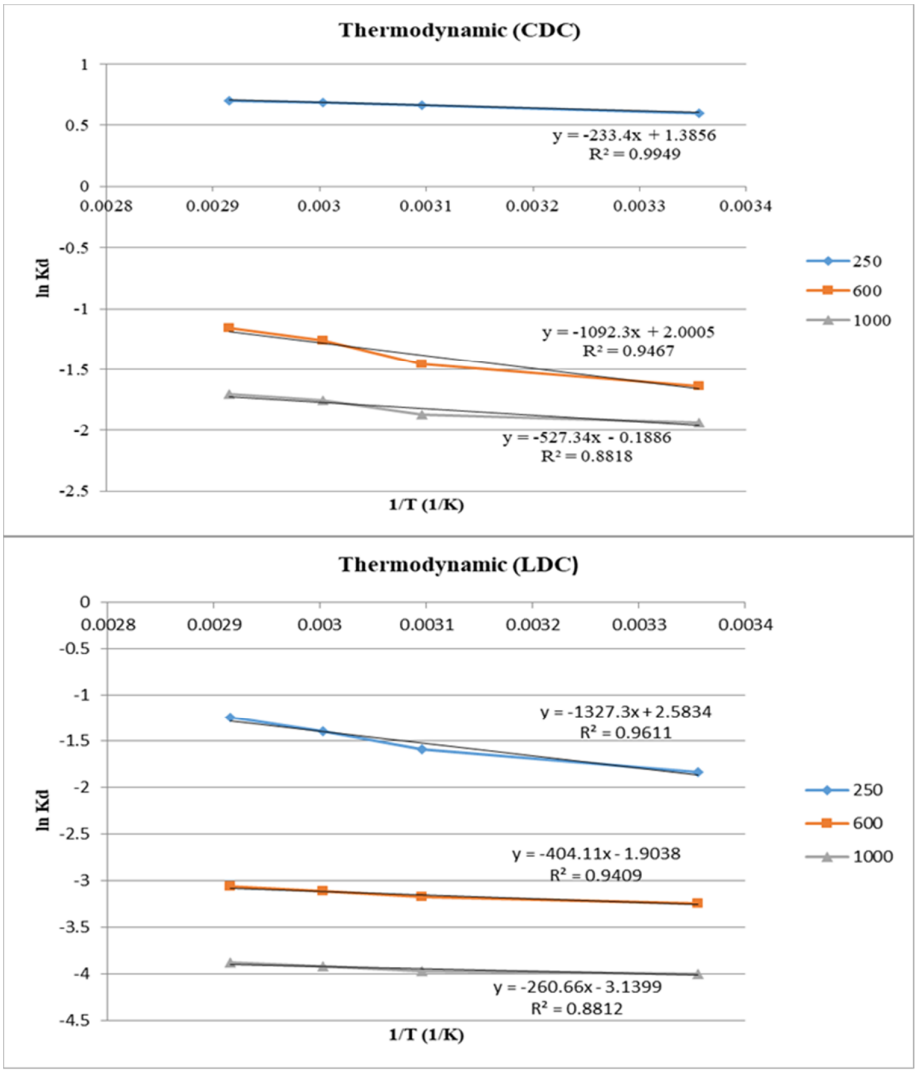

Figure 12. Plot of $\ln K_d$ versus 1/temperature to determine enthalpy and entropy of the adsorption reaction for CDC and LDC (initial chloride concentration: 1000, 600, 250 mg/L, speed stirrer: 500 rpm, temperature: 298 K, 323 K, 333 K, 343 K).

4. Conclusions

In this work, two novel adsorbents were prepared, characterized, and applied for use by the batch adsorption method. The optimized values for the contact time, amount of adsorbent, and pH were found to be 30 min, 1 g, and 7, respectively. The experimental results were fitted to the Langmuir equation, implying a homogeneous (monolayer surface) chloride adsorption. The adsorption quantities from the Langmuir model for CDC and LDC were 63.291 mg/g and 52.356 mg/g at 293 K, respectively.

According to the kinetic studies on both CDC and LDC, chemisorption of adsorptive removal of chloride ions and the presence of film mass transfer and internal diffusion combination in the process were confirmed. In the adsorptive removal of chloride ions onto both CDC and LDC, the film mass transfer factors are more than internal diffusion, which indicates its greater impact on the process.

The ΔG° values at low concentrations indicate that the adsorptive removal of chloride ions by CDC is a spontaneous process. The positive values of ΔG° for LDC indicates that the process is not spontaneous but stirring the solution helps the process to occur. Due to the ΔH° values, it can be confirmed that the adsorptive removal of chloride ions for both adsorbents is endothermic. The calculated values for ΔS° for chloride ion adsorption describes that at low concentrations, chloride ions interact with the adsorbent associatively, and at high concentrations, dissociatively.

www.SID.ir

Archive of SID

As the conclusion, the simplicity of the adsorbent synthesis process along with achieving a high efficiency in the adsorptive removal of chloride ions cause these materials to become an applicable adsorbent in the water treatment process.

Acknowledgement
We are thankful to the Department of Mining Engineering of Science and Research Branch of the Islamic Azad University for their support.

References

[1]. Horii, Y., Higuchi, S., Shimaoka, T. and Hanashima, M. (1997). The treatment technology of landfill leachates containing condensed inorganic salts. Waste Manage. Res. 8: 529–539.

[2]. Kameda, T., Yabuuchi, F., Yoshioka, T., Uchida, M. and Okuwaki, A. (2003). New method of treating dilute mineral acids using magnesium aluminum oxide. Water Res. 37: 1545–1550.

[3]. Kameda, T., Yoshioka, T., Mitsuhashi, T., Uchida, M. and Okuwaki, A. (2003). The simultaneous removal of calcium and chloride ions from calcium chloride solution using magnesium–aluminum oxide. Water Res. 37: 4045–4050.

[4]. Lv, L., He, J., Wei, M., Evans, D.G. and Duan, X. (2006). Uptake of chloride ion from aqueous solution by calcined layered double hydroxides: Equilibrium and kinetic studies. Water Res. 40: 735–743.

[5]. Kameda, T., Miyano, Y., Yoshioka, T., Uchida, M. and Okuwaki, A. (2000). New treatment methods for waste water containing chloride ion using magnesium–aluminum oxide. Chem. Lett. 29: 1136–1137.

[6]. Eaton, A.D., Franson, M.A.H., A.P.H. Association, A.W.W. Association, W.E. and Federation, w.(2005). Standard Methods for the Examination of Water and Wastewater. American Public Health Association, Washington, DC.

[7]. Yao, Y., Xu, F., Chen, M., Xu, Z. and Zhu, Z. (2010). Adsorption behavior of methylene blue on carbon nanotubes. Bioresour. Technol. 101: 3040–3046.

[8]. Apte Sagar, S., Apte Shruti, S. and Kore, V.S. (2011). Chloride Removal from Wastewater by Biosorption with the Plant Biomass. Uni. Jour. of Environ. Res. and Technol. 1 (4): 416-422.

[9]. Agudelo, N., Hinestroza, J.P. and Husser, J. (2016). Removal of sodium and chloride ions from aqueous solutions using fique fibers (Furcraea spp.). Water Sci. & Tech. 73 (5): 1197-1201.

[10]. Iakovleva, E., Makila, E., Salonen, J., Sitarz, M. and Sillanpaa, M. (2015). Industrial products and wastes as adsorbents for sulphate and chloride removal from synthetic alkaline solution and mine process water. Chem. Eng. J. 259: 364-371.

[11]. Mass, E. V. and Ogata, G. (1971). Absorption of Magnesium and Chloride by Excised Corn Roots. Plant Physiol. 47: 357-360

[12]. Shokrian, F., Solaimani, K., Nematzadeh GH. and Biparva, P. (2015). Removal of Nacl from aqueous solutions by using clinoptilolite. Int. J. Farm. and Allied Sci. 4 (1): 50-54.

[13]. Ma, R., Zhu, J., Wu, B. and Li, X. (2016). Adsorptive removal of organic chloride from model jet fuel by Na-LSX zeolite: kinetic, equilibrium and thermodynamic studies. Chem. Eng. Res. and Des. 114: 321-330.

[14]. Osio-Norgaard, J. and Srubar, W.V. (2019). Zeolite Adsorption of Chloride from a Synthetic Alkali-Activated Cement Pore Solution. Material. 12(12): 2019.

[15]. Thakre, D., Rayalu, S., Kawade, R., Meshram, S.. Subrt, J. and Labhsetwar, N. (2010). Magnesium incorporated bentonite clay for defluoridation of drinking water. J. Hazard. Mater., 180: 122–130.

[16]. Masindi, V., Gitari, M.W., Tutuc, H. and De Beer, M. (2014). Application of magnesite_bentonite clay composite as an alternative technology for removal of arsenic from industrial effluents. Tox. & Enviro. Chem. 96(10): 1435-1451.

[17]. Zhang, H., Zhou, J., Muhammad, Y., Tang, R., Liu, K., Zhu, Y. and Tong, Z. (2019). Citric Acid Modified Bentonite for Congo Red Adsorption. Fron. in Mater. 6: 5.

[18]. LI, Z. and BOWMAN, R.S. (2001). Retenition of inorganic oxyanions by organo-kaolinite. Wat. Res. 35(16): 3771–3776.

[19]. Jin, X., Jiang, M., Duc, J. and Chen, Z., (2013). Removal of Cr(VI) from aqueous solution by surfactant-modified kaolinite. J. Ind. and Eng. Chem. 20(5): 3025-3032

[20]. Nabbou, N., Belhachemi, M., Boumelik, M., Merzougui, T., Lahcene, D., Harek, Y., Zorpas, A.A. and Jeguirim, M. (2018). Removal of fluoride from groundwater using natural clay (kaolinite): Optimization of adsorption conditions. Comp. Rend. Chimie, 22: 105-112.

[21]. Meyn, M., Beneke, K. and Lagaly, G. (1990). Anion-exchange reactions of layered double hydroxides. Inorg. Chem. 29 (26): 5201-5207.

[22]. Sarakha, L., Forano, C. and Boutinaud, P. (2009). Intercalation of luminescent Europium (III) complexes in layered double hydroxides. Optical Mate. 31(3): 562-566.

[23]. Fogg, A. M., Green, V. M., Harvey, H. G. and O'Hare, D. (1999). New separation science using

www.SID.ir

Archive of SID

shape-selective ion exchange intercalation chemistry. Advanced Mater. 11(17): 1466.

[24]. Ryu, S.J., Jung, H., Oh, J. M., Lee, J.K. and Choy, J.H. (2010). Layered double hydroxide as novel antibacterial drug delivery system. J. Phys. Chem. Sol. 71 (4): 685-688

[25]. Cornejo, J., Celis, R., Pavlovic, I. and Ulibarri, M. A. (2008). Interactions of pesticides with clays and layered double hydroxides: a review. Clay Minerals, 43 (2), 155.

[26]. Srivastava, B., Jhelum, V., Basu, D.D. and Patanjali, P.K. (2009). Adsorbents for pesticide uptake from contaminated water: A review. J. Sci. and Ind. Res. 68: 839-850.

[27]. Chi, L., Wang, Z., Zhou, Y., Lu, S. and Yao, Y. (2018). Layered Double Hydroxides Precursor as Chloride Inhibitor: Synthesis, Characterization, Assessment of Chloride Adsorption Performance. Material, 11(12): 2537.

[28]. Kamimoto, Y., Okamoto, N., Hagio, T., Yong-Jun, J., Deevanhxay, P. and Ichino, R. (2019). Development of magnesium–iron layered double hydroxide and application to nitrate removal. SN Appl. Sci., 1: 1399.

[29]. Salman, H.E., and Hussein, N.J. (2019). Synthesis of Zinc-Aluminum Layered Double Hydroxides and Application of Adsorption for Nitrate from Water. IOP Conference Series: Mat. Sci. and Eng., 571 (1).

[30]. Liu, C. and Bai, R., (2014). Recent advances in chitosan and its derivatives as adsorbents for removal of pollutants from water and wastewater. Curr. Opin. Chem. Eng. 4: 62–70.

[31]. Sowmya, A. and Meenakshi, S. (2013). An efficient and regenerable quaternary amine modified chitosan beads for the removal of nitrate and phosphate anions. J. Environ. Chem. Eng. 1: 906–915.

[32]. Gupta, V.K., Gupta, M. and Sharma, S. (2001). Process development for the removal of lead and chromium from aqueous solutions using red mud—an aluminium industry waste. Water Res. 35 (5):1125–1134.

[33]. Xie, J., Li, C., Chi, L. and Wu, D. (2013). Chitosan modified zeolite as a versatile adsorbent for the removal of different pollutants from water. Fuel 103: 480–485.

[34]. Kumar M.N.V.R. (2000). A review of chitin and chitosan applications. React. Funct. Polym, 46: 1-27.

[35]. Knorr, D. (1983). Dye Binding Properties of Chitin and Chitosan. J. Food Sci. 48: 36-37.

[36]. Jing, Y., Liu, Q., Yu, X., Xia,W. and Yin, N. (2013). Adsorptive removal of Pb (II) and Cu (II) ions from aqueous solutions by crosslinked chitosan-polyphosphate-epichlorohydrin beads. Sep. Sci. Technol. 48 (14): 2132–2139.

[37]. Khraisheh, M.A., Al-degs, Y.S. and Mcminn, W.A. (2004). Remediation of wastewater containing heavy metals using raw and modified diatomite. Chem. Eng. J. 99 (2): 177–184.

[38]. Chen, J., Yan, L. G., Yu, H.Q., Li, S. Qin, L.L., Liu, G.Q., Li, Y.F. and Du, B. (2016). Efficient removal of phosphate by facile prepared magnetic diatomite and illite clay from aqueous solution. Chem. Eng. J. 287: 162–172.

[39]. Xu, L., Gao, X., Li c, Z. and Gao, C. (2015). Removal of fluoride by nature diatomite from high-fluorine water: An appropriate pretreatment for nanofiltration process. Desalination 369: 97–104.

[40]. Wu, C.C., Wang, Y.C., Lin, T.F., Tsao, H.L. and Chen, P.C. (2006). Removal of arsenic from waste water using surface modified diatomite. J. Chin. Ins. Enviro. Eng. 15 (4): 255-261.

[41]. Khalighi Sheshdeh, R., Khosravi Nikou, M. R., Badii, Kh., Yousefi Limaee, N. and Golkarnarenji, G. (2014). Equilibrium and kinetics studies for the adsorption of Basic Red 46 on nickel oxide nanoparticles-modified diatomite in aqueous solutions. J. Taiw. Inst. Chem. Eng. 45: 1792-1802.

[42]. Zheng, L., Wang, Ch., Shu, Y., Yan, X. and Li, L. (2014). Utilization of Diatomite/chitosan-Fe (III) Composite for the Removal of Anionic Azo Dyes from Wastewater: Equilibrium, Kinetics and Thermodynamics. Colloi. Surf. A: Physicochem. Eng. Aspects. 468 (5): 129-139

[43]. Das, J., Patra, B.S., Baliarsingh, N. and Parida, K. (2006) Adsorption of phosphate by layered double hydroxides in aqueous solutions. Appl. Clay Sci. 32(3/4): 252–260

[44]. Tan, G. and Xiao, D. (2009). Adsorption of cadmium ion from aqueous solution by ground wheat stems. J. Hazard. Mater.,164:1359-1363.

[45]. Chingombe, P., Saha, B. and Wakeman, R. (2006). Sorption of atrazine on conventional and surface modified activated carbons. J. Colloid Interface Sci. 302: 408-416.

[46]. Foo, K. and Hameed, B. (2010). Insights into the modeling of adsorption isotherm systems. Chem. Eng. J. 156: 2-10.

[47]. Crini, G., Peindy, H.N., Gimbert, F. and Robert, C. (2007). Removal of CI Basic Green 4 (Malachite Green) from aqueous solutions by adsorption using cyclodextrin-based adsorbent: Kinetic and equilibrium studies. Sep. Purif. Technol. 53: 97-110.

[48]. Ofomaja, A.E. and Ho, Y.S. (2007). Equilibrium sorption of anionic dye from aqueous solution by palm kernel fibre as sorbent. Dyes Pigm., 74: 60-66.

[49]. Özacar, M. and Şengil, İ.A. (2004). Equilibrium data and process design for adsorption of disperse dyes onto alunite. Environ. Geol. 45: 762-768.

www.SID.ir

Archive of SID

[50]. Özcan, A.S., Gök, Ö. and Özcan, A. (2009). Adsorption of lead (II) ions onto 8-hydroxy quinolineimmobilized bentonite. J. Hazard. Mater., 161:499-509.

[51]. Mall, I.D., Srivastava, V.C., Agarwal, N.K. and Mishra, I.M. (2005). Removal of congo red from aqueous solution by bagasse fly ash and activated carbon: kinetic study and equilibrium isotherm analyses. Chemosphere., 61: 492-501.

[52]. Hobson, J.P. (1969). Physical adsorption isotherms extending from ultrahigh vacuum to vapor pressure. J. Phys. Chem. 73: 2720-2727.

[53]. Doğan, M., Alkan, M., Demirbaş, Ö., Özdemir, Y. and Özmetin, C. (2006). Adsorption kinetics of maxilon blue GRL onto sepiolite from aqueous solutions. Chem. Eng. J. 124: 89-101.

[54]. Hamdaoui, O. (2006). Batch study of liquid-phase adsorption of methylene blue using cedar sawdust and crushed brick, J. Hazard. Mater. 135: 264–273.

[55]. Dog˘an, M. and Alkan, M. (2003). Removal of methyl violet from aqueous solution by perlite, J. Colloid Interface Sci. 267: 32–41.

[56]. Bulut, E., Özacar, M. and Şengil, İ.A. (2008). Adsorption of malachite green onto bentonite: equilibrium and kinetic studies and process design. Microporous Mesoporous Mater. 115:234- 246.

[57]. Ala'a, H., Ibrahim, K.A., Albadarin, A.B., Ali-Khashman, O., Walker, G.M. and Ahmad, M.N. (2011). Remediation of phenol-contaminated water by adsorption using poly (methyl methacrylate) (PMMA). Chem. Eng. J. 168 (2): 691–699.

[58]. Brugnerotto J., Lizardi J., Goycoolea F. M., Argüelles-Monal W., Desbrieeŕes J. and Rinaudo, M. (2001). An infrared investigation in relation with chitin and chitosan characterization. Polymer. 42(8): 3569-3580.

[59]. Hu, Y., Jiang, X., Ding, Y., Ge, H., Yuan, Y. and Yang, C. (2002). Synthesis and characterization of chitosan-poly(acrylic acid) nanoparticles. Biomaterials. 23(15): 3193-3201

[60]. Zaitoon, B., Yousef, R.I. and Musleh, S.M. (2011). Modification of Jordanian Diatomite and Its Use for the Removal of Some Organic Pollutants from Water. Oriental J. Chem. 27 (4): 1357-1374

[61]. Caiots, J, (2000). Interpretation of Infrared Spectra a Practical Approach. edited by Meyers R.A, Encyclopedia of Analytical Chemistry, John Wiley & Sons Ltd, Chichester, 10815-10837.

[62]. Haya Kawa, S. and Hench, L.L. (2000). Study on infrared spectra of silica clusters and modified by fluorine. J. Non- Crystalline solids. 262 (1-3): 264 - 270.

[63]. Lu, H.T., Zhu, Z.L., Zhang, H., Zhu, J.Y. and Qiu, Y.L. (2015). Simultaneous removal of arsenate and antimonite in simulated and practical water samples by adsorption onto Zn/Fe layered double hydroxide. Chem. Eng. J. 276: 365-375.

[64]. Fan, D.X., Jia, L., Xiang, H.Y., Peng, M.J., Li, H. and Shi, S.Y. (2017). Synthesis and characterization of hollow porous molecular imprinted polymers for the selective extraction and determination of caffeic acid in fruit samples. Food Chem. 224: 32-36.

[65]. Chaisena, A. and Rangsriwatananon, K. (2005). Synthesis of sodium zeolites from natural and modified diatomite. Mater Lett. 59 (12):1474–1479.

[66]. Bangyekan, C., Aht-Ong, D. and Srikulkit, K. (2006). Preparation and properties evaluation of chitosan-coated cassava starch films. Carbohydrate Polymers. 63 (1): 61-71.

[67]. Zhu, J.Y., Zhu, Z.L., Zhang, H., Lu, H.T., Zhang, W., Qiu, Y.L., Zhu, L.Y. and Küppers, S. (2018). Calcined layered double hydroxides/reduced grapheme oxide composites with improved photocatalytic degradation of paracetamol and efficient oxidation-adsorption of As (III). Appl. Catal. B: Environ. 225: 550-562.

[68]. Gu, N., Gao, J.L., Wang, K.T., Li, B., Dong, W.C. and Ma, Y.L. (2016). Microcystis aeruginosa inhibition by Zn-Fe-LDHs as photocatalyst under visible light. J. Taiwan Inst. Chem. E. 64: 189-195.

[69]. Al-Degs, Y.S., El-Barghouthi, M.I., El-Sheikh, A.H.. and Walker, G.M. (2008). Effect of solution pH, ionic strength, and temperature on adsorption behavior of reactive dyes on activated carbon. Dyes Pigm. 77 (1): 16–23.

[70]. Hameed, B., Tan, I. and Ahmad, A. (2008) Adsorption isotherm, kinetic modeling and mechanism of 2, 4, 6- trichlorophenol on coconut husk-based activated carbon. Chem. Eng. J. 144 (2): 235–244.

[71]. Doğan, M., Alkan, M., Demirbaş, Ö., Özdemir, Y. and Özmetin, C. (2004). J. Hazard. Mater. 109: 141–148.

www.SID.ir

Archive of SID

بررسی مقایسه‌ای و رقابتی LDH/دیاتومیت و کیتوسان/دیاتومیت برای جذب یون‌های کلراید از محلول‌های آبی

فرزین صدوق عباسیان[1]، بهرام رضایی[2*]، امیر رضا آزادمهر[2] و هادی حمیدیان شورمستی[3]

1- بخش مهندسی معدن، دانشگاه آزاد اسلامی واحد علوم و تحقیقات، تهران، ایران
2- بخش مهندسی معدن و متالورژی، دانشگاه صنعتی امیرکبیر، تهران، ایران
3- بخش مهندسی معدن، دانشگاه آزاد اسلامی واحد قائمشهر، قائمشهر، ایران

ارسال 2019/10/13، پذیرش 2020/1/7

* نویسنده مسئول مکاتبات: rezai@aut.ac.ir

چکیده:

در این تحقیق، دو کامپوزیت پایه رسی برای جذب یون‌های کلراید از محیط آبی تهیه گردیده است. این کامپوزیت‌ها از طریق آنالیزهای طیف‌سنجی مادون‌قرمز، میکروسکوپ الکترونی، فلوئورسانس اشعه ایکس و پراش اشعه ایکس صورت پذیرفت. تأثیر پارامتر هایی چون زمان تماس، میزان جاذب، غلظت کلراید، دما و pH با استفاده از آزمایش‌های ناپیوسته مورد مطالعه قرارگرفت. همچنین مطالعات ایزوترم، سینتیک و ترمودینامیک جذب یون‌های کلراید توسط دو کامپوزیت بررسی گردید. با توجه به نتایج بدست آمده، جذب یون‌های کلراید در ابتدا سریع و پس از 30 دقیقه به زمان تعادل رسید. مقدار بهینه pH برای جذب بهتر برابر با 7 بود و بیشترین میزان ظرفیت جذب برای غلظت اولیه کلراید 1000 میلی گرم بر لیتر به میزان 60/2 میلی گرم بر گرم بدست آمد. مدل‌های جذب لانگمویر، فرندلیچ، تمکین و دوبنین رادوشکویچ برای توصیف ایزوترم‌های جذب در غلظت‌های مختلف کلراید استفاده گردید. طبق ایزوترم‌های جذب و ضرایب همبستگی (R^2_{CDC}: 0/9424 و R^2_{LDC}: 0/996)، فرآیند توسط مدل لانگمویر قابل توصیف است و بیشترین نرخ حذف، 97/24 درصد (24/31 میلی گرم بر گرم) برای غلظت اولیه کلراید به میزان 250 میلی گرم در لیتر را نشان می دهد. برای شناسایی مکانیزم جذب یون‌های کلراید مدل‌های سینتیک جذب شبه مرتبه اول، شبه مرتبه دوم، نفوذ درون ذره‌ای و انتقال جرم مورد استفاده قرارگرفت. طبق ضرایب همبستگی (R^2_{CDC}: 0/9217-0/9852 و R^2_{LDC}: 0/9227-0/9926) مدل شبه مرتبه دوم با محاسبات سینتیکی مطابقت دارد و این مدل برای فرآیند جذب یون کلراید توسط جاذب‌ها کاربرد دارد. محاسبات ترمودینامیکی نشان می‌دهد که در غلظت پایین کلراید، فرآیند خود به خودی، با افزایش بی‌نظمی و گرماگیر است. در غلظت‌های بالا فرآیند غیر خود به خودی، با کاهش بی‌نظمی و گرماگیر است. میزان انرژی آزاد جذب (E) محاسبه شده برای جاذب‌ها به این موضوع اشاره دارد که فرآیند بیشتر توسط سرعت واکنش نسبت به نفوذ کنترل می‌گردد. می‌توان نتیجه گرفت دو کامپوزیت قابلیت استفاده به عنوان دو جاذب موثر و کاربردی برای جذب یون‌های کلراید را دارند.

کلمات کلیدی: جذب، پساب، کلراید، تبادل آنیونی، دیاتومیت.

www.SID.ir